ISSN 2070-2051, Protection of Metals and Physical Chemistry of Surfaces, 2010, Vol. 46, No. 1, pp. 110–116. © Pleiades Publishing, Ltd., 2010.

NEW SUBSTANCES, MATERIALS AND COATINGS

Electrochemical Synthesis of Polypyrrole on Aluminium in Different Anions and Corrosion Protection of Aluminium[1]

S. Zor[a], F. Kandemirli[a], E. Yakar[a], and T. Arslan[b]

[a] *Kocaeli University Science & Art Faculty, Chemistry Department, 41380 Kocaeli, Turkey*

[b] *Eskisehir Osmangazi University, Science&Art Faculty, Chemistry Department, 26480, Eskisehir, Turkey*

e-mail: merve@kou.edu.tr, szor2001@yahoo.com

Received August 26, 2008

Abstract—In this study, polypyrrole was deposited on the aluminium in different anions (CO_3^{2-}, NO_2^-, CrO_4^{2-}, DBS^-). The contribution of anions to formation of polypyrrole film was investigated by using cyclic voltammetry (CV) technique. The effect of polypyrrole film on the corrosion of aluminium was searched in 0.1 M HCI solution by using potentiostatic method. For this purpose, polarization curves were obtained, corrosion current density (icorr), corrosion potential (Ecorr), polarization resistance (Rp) were determined from the polarization curves. Moreover, the percent efficiency of coating was calculated. The complexes of pyrrole pentamers and different anions (CO_3^{2-}, NO_2^-, CrO_4^{2-}, DBS^-) were studied using ab initio quantum chemical at the Hartree-Fock (HF) levels with STO-3G, 3-21G, 6-31G(d,p) [13] basis sets and HOMO-LUMO energy gap is calculated by B3LYP method with 3-21G* and 6-31G(d,p) basis sets. The polypyrrole film obtained in CrO_4^{2-} anion is determined to be the most effective in prevention to pitting corrosion of aluminium as experimental and theoretical.

DOI: 10.1134/S2070205110010168

1. INTRODUCTION

The electrically conductive polymers drive quite more attention in recent years due to their electronic characteristics. Especially, works on conductive polymers coating on the surface of iron, steel, zinc, aluminum and other oxidizing metals are very hopeful [1–8]. The mostly used polymers in these works are polyaniline [1, 2], polypyrrole [2–4], polythiophene [9] and polyindole [10]. Conductive polymers have many advantages such as environmental stability, having no toxic effect, the state of controllable conductive oxidation, easy and economic supply. The conductive polymers can easily be obtained in media with dilute and/or organic dissolver by using electrochemical techniques [1–12]. The mostly used conductive polymers have been proven to be efficient as protective films against corrosion of metals in so far as they produce a galvanic effect characterized as an anodic protection where the oxidizing power of the CP is able to set the metal in the passive state [12].

The conductivity of polymers can be changed by chemical or electrochemical ways. This process, carried on with reduction or oxidation is named as doping. The solubility increases and the oxidation potential of monomer decreases in the media where doping takes place. Considering this mechanism, many conductive polymers are synthesized in dilute mediea electrically by using different anions [1–8]. The characteristics of conducting polymers strongly depend on their polymerization condition such as the film growth rate, the nature of solvent and kind and concentration of dopant anion [11–14]. The natures of the anions used in doping are also important. The anions used in electrosynthesis and electrochemical polymerization are divided into three groups: 1) small inorganic anions: such as Cl^-, Br^-, ClO_4^-, NO_3^-, BF_4^-, 2) medium sized (mainly organic) anions: benzenesulfonate, dodecylsulfonate, 3) large polymeric anions such as polyvinylsulfonate, polystyrenesulfonate. The mobility of the anions in polymer films changes with the size of the anions. Small anions have better mobility than the bigger ones. The mobility of big size anions are less. The nature of the solvent also has been gained importance at anion mobility [15].

The electrochemical redox behavior of the polypyrrole films doped with benzenesulfonate was investigated by cyclic voltammetry, the surface morphology of the films was characterized by AFM, and the interactions between pyrrole oligomers and the benzenesulfonate anion were modeled with quantum chemical methods [22]. The vibrational spectra of isolated pyr-

[1] The article is published in the original.

role monomers and oligomers have been computed using the ab initio 3-21G basis set [23]. The stabilization energies of pyrrole pentamer dications with the $ClO_4^- < Br^- < Cl^- NO_3^-$ anions calculated using AM1, HF/6-31G(d) methods and According to quantum chemical calculations, the interaction of sulfate anions with oligopyrrole dications is about twice as large as that of the singly charged anions [24].

In this study, polypyrrole films were synthesized electrochemically in different anions (CO_3^{2-}, NO_2^-, CrO_4^{2-}, DBS^-) by using cyclic voltammetry technique and quantum chemical calculations were done for pyrrole pentamer dications with the CO_3^{2-}, NO_2^-, CrO_4^{2-}, DBS^- DBS^- anions at the Hartree-Fock (HF) levels with. STO-3G, 3-21G 6-31G(d,p) basis sets and HOMO-LUMO energy gap for trimer dications with the CO_3^{2-}, NO_2^-, CrO_4^{2-}, DBS^- DBS^- anions were calculated by B3LYP method with 3-21G* and 6-31G(d,p) basis sets. The effect of polypyrrole film on the corrosion of aluminium in 0.1 M HCI solution is searched by using potensiostatic polarization method.

2. EXPERIMENTAL

2.1. Electrochemical Method

All the chemicals used in electrochemical measurements were bought from Aldrich Chemical Company and purification was not done. All the solutions were prepared with bidistilled water. The measurements were done in room temperature.

The electrochemical measurements were done by using three electrode techniques. Pt wire was used as opposite electrode, Saturated Calomel Electrode (SCE) as reference electrode and aluminum electrode as working electrode. The working electrode was of 99.5% pure aluminum in disc form the surface except for those contacting solution were coated with polytetraflouroethylene (PTFE). The surface of the working electrode was 0.785 cm^2. After every measurement, the surface of the working electrode was grounded with 400, 800 and 1200 mesh emery paper until the surface becomes as shiny as mirror. After that, it was washed with acetone and distilled water and transferred to electrochemical cell. All the potentials were measured against the saturated calomel electrode (SCE).

The electrochemical measurements were done by using EG&G PAR Model 263A Potentiostat/Galvanostat device. For electropolymerization of PPy, cyclic voltametry technique was used, with Cyclic voltametry, electrochemical coating process was carried on between potential ranges of (−1.0 V)−(3.0 V) at 50 mV/s scanning rate as a result of 30 cyclic scanning. The monomer concentration was kept at 0.1 M. In doping, 0.1 M Na_2CO_3, 0.1 M $NaNO_2$, 0.1 M Na_2CrO_4, 0.1 M NaDBS solutions were used. Solutions were mixed in the magnetic mixer for 30 minutes to be balanced. After the coated aluminum samples were washed with distilled water and dried, the potentiodynamic polarization measurements were done in 0.1 M HC1 at scanning rate of 10 mV/s. Electrochemical parameters were determined from the polarization curves.

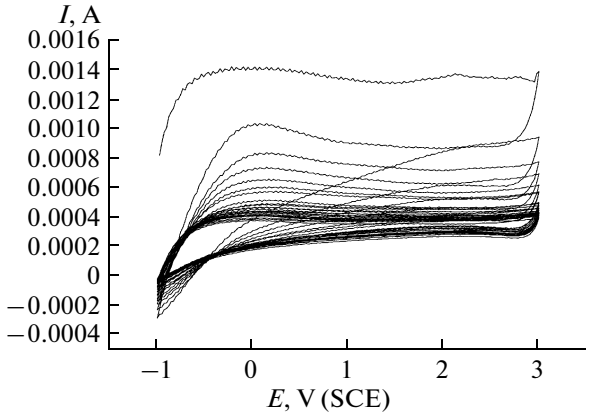

Fig. 1. Cyclic voltammograms of the PPy films deposited on Al in 0.1 M Na_2CO_3 50 mV/s (30 cycle).

2.2. Method of Calculations

Theoretical calculations were carried out at the Hartree-Fock (RHF) and B3LYP level using the standard Gaussian 03 (Revision B.05) software package [25] with STO-3G, 3-21G 6-31G(d,p) basis sets [26–29].

3. RESULTS AND DISCUSSION

3.1. Cyclic Voltammetry Results

The dopant effect of different anions (CO_3^{2-}, NO_2^-, CrO_4^{2-}, DBS^- DBS) in the electropolymerization of polypyrrole was investigated by using cyclic voltametry. The surface of the aluminum was coated with a polymer by adding 0.1 M monomer (pyrrole) to solutions consisting of 0,1 M anion, at a 50 mV/s scanning rate, at a potential range of (−1.0 V) − (+3.0 V) (SCE) by 30 scans.

The PPy $|CO_3^{-2}|$ Al and PPy $|NP_2^-|$ Al cyclic voltammograms are shown in Fig. 1 and Fig. 2 respectively. A wide and scattered wave is obtained in the first scanning. Because of the oxidation of aluminum ions, the current increases with further scans. In reverse scanning, the current decreases due to the formation of Al_2O_3 on the surface and on the polymer film. Hydrogen oxidation peak is obtained at 0.0 V (Figs. 1, 2). As the number of scans increases, the oxidation peak of hydrogen disappears (Figs. 1, 2). As the number of the scans increases, the thickness of the polymer films

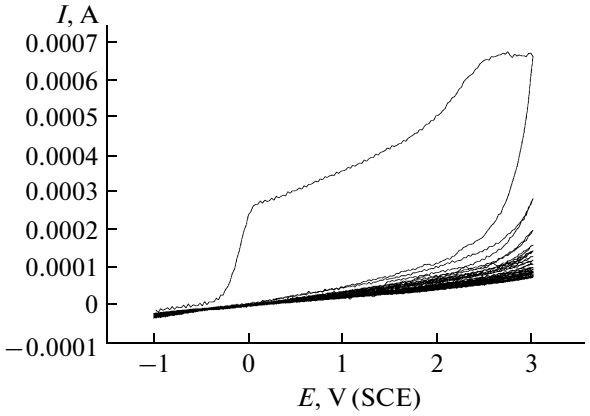

Fig. 2. Cyclic voltammograms of the PPy films deposited on Al in 0.1 M $NaNO_2$ 50 mV/s (30 cycle).

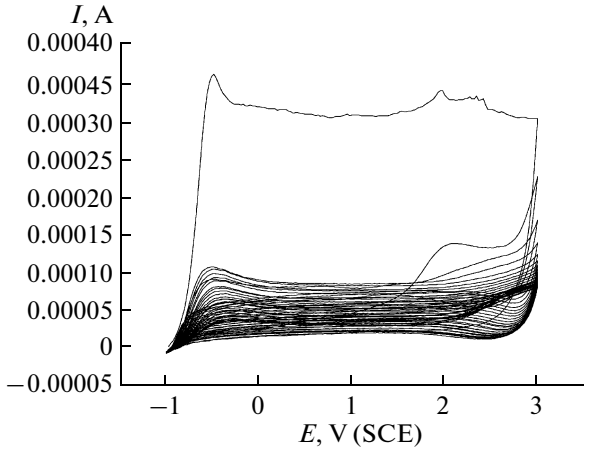

Fig. 3. Cyclic voltammograms of the PPy films deposited on Al in 0.1 M Na_2CrO_4 50 mV/s (30 cycle).

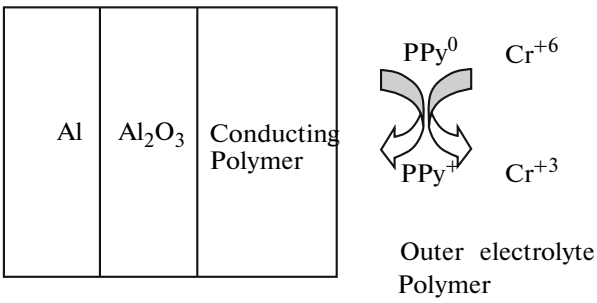

Fig. 4. The schematic representation of the reduction of CrO_4^{2-} anions within the outer layers of the polymer film on aluminium electrode surface.

increases and the current decreases. At the 30th scan, the current amplitude becomes less and it approaches 0.0 A (Figs. 1, 2).The surface became coated with black color PPy film at the end of the 30th cycle. It must be noted that the repassivation peak disappeared, since the surface was covered with polymer film and the interaction of aluminum was prevented with the electrolyte solution. At the same time, the polymer film was formed by the electrostatic interactions between anions and positive charge centers of the polymer chain. This situation was related to oxidation behavior of polymer film, which could be represented as given below;

$$PPy^+ + nyA^- \longrightarrow (PPy^+A_y)_n + 2ny\bar{e}\,.$$

The PPy $|CrO_4^{2-}|$ Al cyclic voltammogram is given in Fig. 3. At the first cycle, a wider current wave can be observed in PPy $|CrO_4^{2-}|$ Al. At −0.5 V, the oxidation peak occurs and at 2.0 V the reduction peak occurs. With the reduction of Cr^{+6} to Cr^{+3}, the reduction peaks occur (Fig. 3). As shown in Fig. 4, the CrO_4^{2-} anions may be reduced also within the outer layers of the polymer film [16]. At the polymer-solution interface, a direct electron transfer between the PPy and Cr (VI) results in the reduction of hexavalent chromium to the trivalent state (as Cr_2O_3). According to this [16]:

$$CrO_4^{2-} + 8H^+ + PPy^0 \longrightarrow 2Cr^{+3} + 6PPy^+ + 4H_2O.$$

The chromate anions adsorbed by the surface during electropolymerization are reduced to the more stable configuration of trivalent chromium and form Cr (III) oxide. Having Al_2O_3, the polymer film and Cr_2O_3 together increases the polymer filmÕs thickness. In this way, it is thought that a firmer and more protective layer of film is formed. In the second scan, the current is decreased from 0.37 mA to 0.1 mA due to the deposit of Cr (III) oxide and the polymer film on the surface of the electrode.

The PPy coating obtained by doping with CrO_4^{2-} shows more protective features than the coating with other anions (Fig. 3, 6). The potentiostatic results obtained also support this (Table 1). As the number of scans increases, the thickness of the polymer film increases (Fig. 3). Therefore, the current decreases.

In Fig. 5, the PPy $|DBS^-|$ Al cyclic voltammogram curve is shown. While the current increases in further scans, it decreases in backward scanning. As the number of scans increases, the polymer films formation increases and the current decreases (Fig. 5). The DBS^- anion, being wider than the others, till shows a surface active feature (surfactant). Anodic surfactants, such as SDBS, form micelles (in solution) a bilayered micelles (on electrode surfaces) in aqueous solutions when the surfactant concentration is above the critical micelle concentration (cmc). The value of cmc for SDBS in aqueous solution is as low as 1.6 mM at 25°C [18]. It is thought that rectangular micelles form easily on aluminum electrodes because of the influence of hydrophilic oxide layers on the electrode surface. Pyrrole monomer is considered to be preferentially dissolved and concentrated into the micellar assembly

due to the hydrophobic nature of pyrrole [18]. At the same time, the micellar media affects the electrochemical reaction through an irreversible adsorption, leading to a change in the solution- electrode interface properties [17, 18]. According to this, as a result of having electrostatic interaction between the sulphonate group and the positive charge center at polymer chain, the DBS^- anion is adsorbed irreversibly and covers the electrode surface [19].

In all the cyclic voltammogram curves, the oxidation peak of PPy can not clearly be seen (Figs. 1–5). This is because the polymer film electrosythesized on aluminum is a bilayer film composed of a barrier type Al_2O_3 [18, 19]. The electron transport during the simultaneous electrochemical formation of the Al_2O_3 | Polymer films on the Al electrode is given in Fig. 6 [18, 19]. As shown in Fig. 6, the formation of Al_2O_3 proceeds at two interfaces, namely at the Al | $A1_2O_3$ and at the Al_2O_3 | polymer. That is, as a result of the aluminum surface being covered by a porous Al_2O_3 layer, a polymer coating forms on Al_2O_3. Therefore, the electron transfer can not clearly be seen during the oxidation of PPy (Figs. 1–5). During PPy electropolymerization, the formation of hydrogen in the cathodic reaction decreases due to the electrode surface being covered by a polymer film.

3.2. Corrosion Behavior

The corrosion performance of polypyrrole coated aluminum and uncoated aluminum are studied in 0.1 M HCl solution. The polarization curves for coated ($PPy|CO_3^{2-}|Al$, $PPy|NO_2^-|Al$) and uncoated Al electrodes are shown in Fig. 7.

The anodic and the cathodic current densities decrease in aluminum coated by compared to the uncoated aluminum. This decrease can be attributed to the coating, which prevents the formation of anodic and cathodic reactions by covering the electrode surfaces with a polymer film.

The electrochemical parameters (corrosion current intensity (icorr), corrosion potential (Ecorr), resistance of polarization (Rp), coating efficiency (% CE)) are determined from the polarization curves given in Table 1. The coating efficiency, in %, given in Table 1 is calculated as follows:

$$\textit{Efficiency of coating(EC)} = \frac{(\text{Icorr})\text{uncoated} - (\text{Icorr})\text{coated}}{(\text{Icorr})\text{uncoated}} \times 100$$

(Icorr) uncoated, corrosion current density of uncoated aluminum, (Icorr) coated, corrosion current density of coated aluminum.

It is clear from Table 1 that the corrosion potential of PPy | Anion | Al increases and the corrosion current density decreases sharply. These results indicate that PPy | Anion can act as a protective layer on aluminum and improve the overall corrosion performance. The polarization curves demonstrate that the PPy films cause a positive displacement in the corrosion potential, relative to the value of the uncoated aluminum electrode. This positive displacement of the coated aluminum is higher than that of uncoated aluminum.

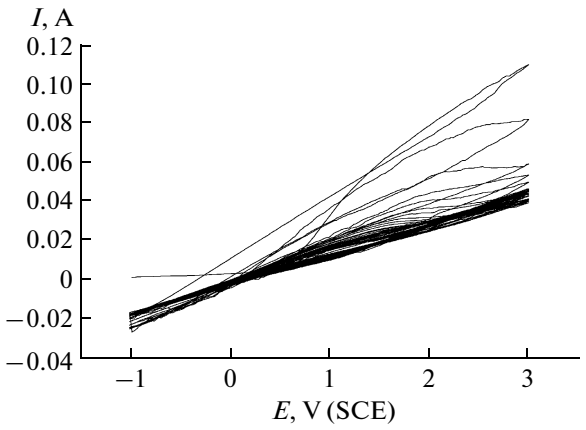

Fig. 5. Cyclic voltammograms of the PPy films deposited on Al in 0.1 M NaDBS 50 mV/s (30 cycle).

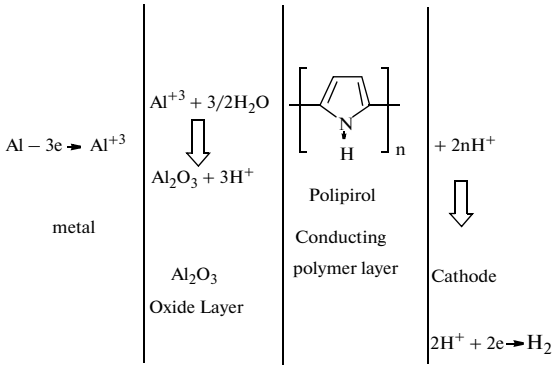

Fig. 6. The schematic representation of the electrochemical formation of Al_2O_3 polymer film.

Table 1. Electrochemical parameters for coated and uncoated aluminum in 0.1 M HC1

Uncoated Al			Icorr, mA/cm^2	Ecorr, mV	Rp, ohm	Percent of efficiency coating
			391.1	−754.8	8818.9	
PPy	NO_2^-	Al	36.1	−643.9	1044.4	90.7
PPy	CO_3^{2-}	Al	31.1	−606.1	1211.9	92
PPy	CrO_4^{2-}	Al	4.076	−644.9	9609.5	99
PPy	DBS^-	Al	54.71	−569.3	627.3	86

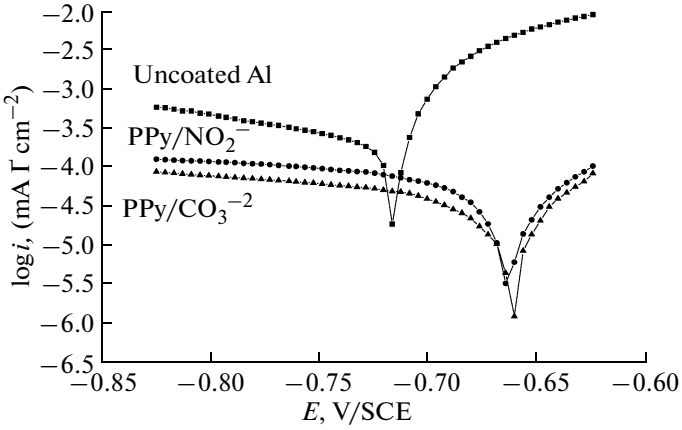

Fig. 7. Polarization curves of aluminium in 0.1 M HCl a) uncoated Al, b) PPy $|CO_3^{2-}|$ Al, c)PPy $|NO_2^-|$ Al.

By using different anions as dopants, the corrosion rate of aluminum coated with PPy decreases notably compared to uncoated aluminum (Table 1). This case was simply related to physical barrier behavior of polymer coating between the corrosive environment and underlying metal. It has limited the transportation of corrosive species to metal surface, effectively. According to this, it is thought that hard and protective PPy films are formed on the electrode surfaces.

The most efficient PPy coating for decreasing the aluminum corrosion rate is obtained for CrO_4^{2-}. The efficiency of the coating is obtained as 99% in PPy (Table 1). According to this, as shown below, Cr (III) oxide forms on electrode surfaces through the cathodic reaction of the chromate anions that are adsorbed by the electrode surface during electropolymerization [20, 21].

$$2Al + 3H_2O \longrightarrow Al_2O_3 + 6H^+ 6e,$$

$$CrO_4^{2-} + 8H^+ + 6e \longrightarrow Cr_2O_3 + 4H_2O.$$

In the formation of the polymer film, the formation of Cr(III) oxide has provided a better protection through thickening the film.

Consequently, the significant decrease in the corrosion rate of aluminum with the PPy film occurred with different anions that prevent the transition of Cl^- ions to the metal surface.

3.3. Theoretical Results

Optimized geometries of anion (CO_3^{2-}, NO_2^-, CrO_4^{2-}, DBS^-) complexes of pentamer dication are given in Fig. 8.

The optimal length of the pentamer dication for the complex formation with different anions (CO_3^{2-}, NO_2^-, CrO_4^{2-}, DBS^-) were determined by HF using STO-3G, 3-21G 6-31G(d,p) basis sets. Complexation energies of the complexes of pentamer dications for optimum length are given in Table 2.

The complexation energy may be found by subtracting the separately calculated energies of the oligomer dication and the anion from the energy of the complex (Eq. (1)):

$$E_{comlexation} = E_{complex} - (E_{oligomer\text{-}dication} + E_{anion}). \quad (1)$$

The complexation energies of pyrrole pentamer dications are given in Table 2 for CO_3^{2-}, NO_2^-, CrO_4^{2-}, DBS^- anions at the Hartree-Fock (HF) levels with STO-3G, 3-21G, 6-31G(d,p) basis sets. All of these methods agree that CrO_4^{2-} ion has the most interaction with pyrrole pentamer dications and DBS^- is the least interaction with the oligomer. The good correlations were obtained between the calculated complexation energies and experimental percent of efficiency coating (Fig. 9). Correlation coefficient val-

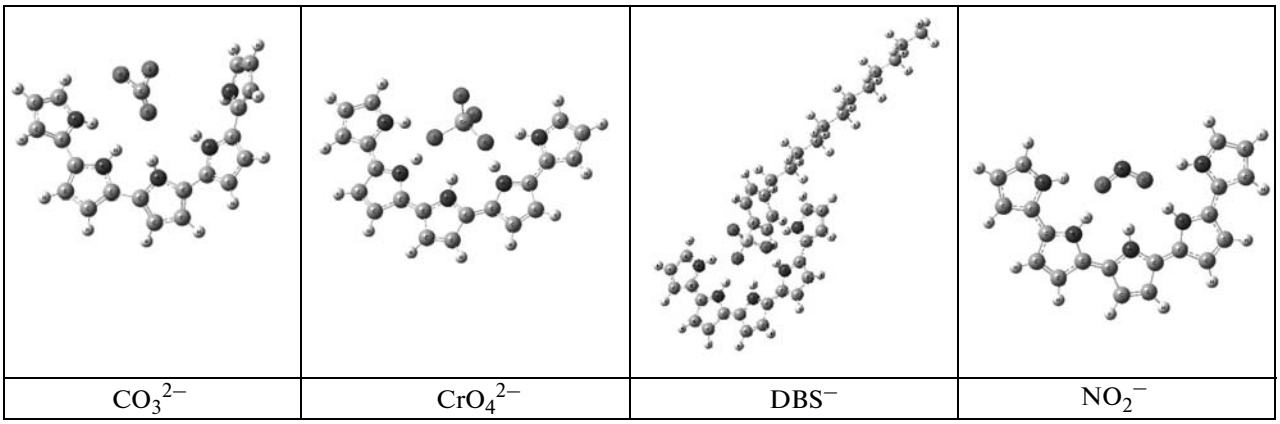

Fig. 8. Optimized of anion (CO_3^{2-}, NO_2^-, CrO_4^{2-}, DBS^-) complexes of pentamer dication with RHF/6-31(d,p).

Table 2. Complexation energies (Kcal/mol) of anions (CO_3^{2-}, NO_2^-, CrO_4^{2-}, DBS^-) with pyrrole pentamer dication, calculate at RHF level with STO-3G, 3-21G, 6-31 G(d,p) parameters

	Complexation energies		
Anions	STO-3G	3-21G	6-31G(d,p)
CO_3^{2-}	−548.664	−363.562	−334.270
DBS^-	−226.820	−213.604	−180.803
CrO_4^{2-}	–	−399.043	−361.068
NO_2^-	−213.895	−221.695	−193.625

Table 3. The energy gap (eV) between LUMO and HOMO for anions (CO_3^{2-}, NO_2^-, CrO_4^{2-}, DBS^-) with pyrrole pentamer dication, calculated with RHF/STO-3G, RHF/3-21G, 6-31G(d,p) and the energy gap (eV) for anions (CO_3^{2-}, NO_2^-, CrO_4^{2-}, DBS^-) with trimer dication, calculated with B3LYP/3-21G*, 6-31G(d,p)

Method/anions	CO_3^{2-}	CrO_4^{2-}	DBS^-	NO_2^-
RHF/STO-3G	10.16489	–	6.79963	6.54575
RHF/3-21G	6.97106	5.91226	5.98437	5.96424
RHF/6-31G(d,p)	8.27994	6.03662	6.13431	6.11254
B3LYP/3-21G*	0.57253	2.49122	2.63340	1.88168
B3LYP/6-31G(d,p)	0.54967	2.43979	2.49422	1.21826

ues were found 72.5% for HF/6-31 G (d, p) and 71.2% for HF/3-21G levels for all molecules.

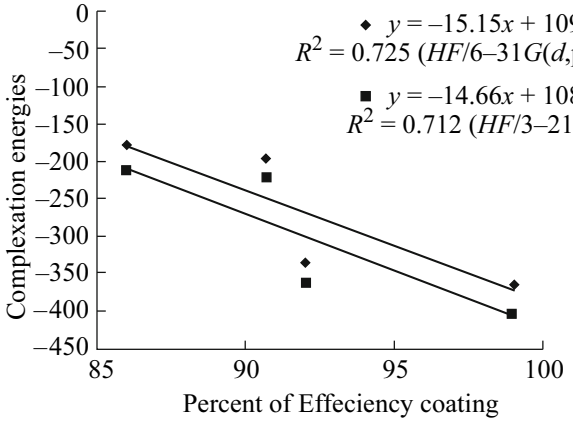

Fig 9. The correlation graphic between calculated complexation energies and experimental percent of efficiency coating.

The reactive ability of the inhibitor is closely related to their frontier molecular orbitals. (MO) and also energy gap between LUMO and HOMO ($\Delta E = E_{LUMO} - E_{HOMO}$) HOMO–LUMO energies were calculated according to length of the pentamer dication for the complex formation with different anions at the Hartree-Fock (HF) levels with STO-3G, 3-21G, 6-31G(d,p) basis sets and B3LYP levels with STO-3G, 3-21G, 6-31G(d,p) basis sets. As seen from the Table 3 Energy gap calculated by using HF level is much higher than calculated by B3LYP level. Energy gap calculated B3LYP with 3-21G* basis set for pyrrole trimer dications with different anions (CO_3^{2-}, CrO_4^{2-}, DBS^-, NO_2^-) are 0.57 eV, 2.49 eV, 2.53 eV, 1.88 eV. The energy gap for the polypyrrole film obtained in CrO_4^{2-} anion is found to be the most biggest and determined the most effective in preventing to pitting corrosion of aluminium.

CONCLUSIONS

Aluminum is coated with PPy in different anions by using the cyclic voltammetry technique. After 30 scans using a scanning rate of 50 mV/s, and a potential range of (−1 V)–(3.0 V) an adhesive and hard PPy coating is obtained on aluminum. The most protective coating was achieved in the CrO_4^{2-} anion.

The anti-corrosive properties of the PPy coatings obtained in different anions were studied in 0.1 M HCl solution, using potentiodynamic polarization measurements.

It is determined that the PPy coating formed in the CrO_4^{2-} anion is more effective in preventing the corrosion of aluminum compared to other anions.

The polypyrrole film obtained in CrO_4^{2-} anion is determined to be the most effective in prevention to pitting corrosion of aluminium as experimental and quantum chemical calculations.

From the cyclic voltametry and potentiostatic and quantum chemical results, it was determined that the PPy coating which was obtained with the CrO_4^{2-} anion was more effective than the other anions in decreasing the corrosion rate of aluminum in 0.1 M HCl.

ACKNOWLEDGMENTS

This study was supported by Research Fund of Kocaeli University. (Project No. 2005/63)

REFERENCES

1. Huerta-Vilca, D., Retina de Moraes, S., and Jesus Motheo, A., *J. Solid State Electrochem.*, 2005, vol. 9, P. 416.
2. Conroy, K.G. and Breslin, C.B., *Electrochim. Acta*, 2003, vol. 48, p. 721.
3. Smitha Akundy, G. and Iroh, J.O., *Polymer.*, 2001, vol. 42, p. 9665.
4. Beck, F. and Hülser, P., *J. Electroanal. Chem.*, 1990, vol. 280, p. 159.
5. Hülser, P. and Beck, F., *J. Apply. Electrochem.,* 1990, vol. 20, p. 596.
6. Naoi, K., Takeda, M., and Kano, H., et al., *Electrochim. Acta.*, 2000, vol. 45, p. 3413.
7. Saidman, S.B. and Bessone, J.B., *J. Electroanal. Chem.,* 2002, vol. 521, p. 87.
8. Zor, S. and Yakar, E., *J.Chem. Soc. Pak* (in press).
9. Kousik, G., Pitchumani, S., and Renganathan, N.G., *Prog. Org. Coat.*, 2001, vol. 43, p. 286.
10. Tuken, T., Yazici, B., and Erbil, M., *Surface and Coatings Technology*, vol. 200(16–17), p. 4802.
11. Lee, K., Yang, K., and Kwak, J., *Electrochem. Comm.*, 2002, vol. 4, p. 128.
12. Hien, N.T.L., Garcia, B., Pailleret, A., and Deslouis, C., *Electrochim. Acta*, 2005, vol. 50, p. 1747.
13. Osaka, T., Naoi, K., Sakai, H., and Ogano, S., *J. Electrochem. Soc.*, 1987, vol. 134, p. 285.
14. Kanamura, K., Kawai, Y., Yonezawa, S., and Takehara, Z., *J. Phys. Chem.*, 1994, vol. 98, p. 2174.
15. Johanson, U., Marandi, M., Tamm, T., and Tamm, J., *Electrochim. Acta*, 2005, vol. 50, p. 1523.
16. Conroy, K.G. and Breslin, C.B., *J. Appl. Electrochem.*, 2004, vol. 34, p. 191.
17. Branzoi, F., *Mol. Cryst. Liq. Cryst.*, vol. 416, p. 73.
18. Naoi, K., Takeda, M., Kano, H., et al., *Electrochim. Acta*, 2000, vol. 45, p. 3413.
19. Fenelon, A.M. and Breslin, C.B., *Synthetic Metals*, 2004, vol. 144, p. 125.
20. Kendig, M., Jeanjaquet, S., Addison, R., and Waldrop, J., *Surface @& Coatings Technology*, 2001, vol. 140, p. 58.
21. Kendig, M., Davenport, A., and Isaacs, H., *Corrosion Sci.*, 1993, vol. 34(1), p. 41.
22. Tamm, J., Raudsepp, T., Marandi, M., and Tamm, T., *Synthetic Metals*, 2007, vol. 157, p. 66.
23. Rabias, L. and Howlin, B.J., *Polymer Science*, vol. 11, p. 241.
24. Johanson, U., Marandi, M., Tamm, T., and Tamm, J., *Electrochim. Acta,* 2005, vol. 50, p. 1523.
25. Frisch, M.J., Trucks, G.W., Schlegel, K.B., et al., *Gaussian 03, Revision B.05.*, Wallingford CT: Gaussian, Inc., 2004.
26. McLean, A.D. and Chandler, G.S., *J. Chem. Phys.,* 1980, vol. 72, p. 5639.
27. McGrath, M.P. and Radom, L., *J. Chem. Phys.,* 1991, vol. 94, p. 511.
28. Bartlett, R.J., *Ann. Rev. Phys. Chem.,* 1981, vol. 32, p. 359.
29. Young, D.C., *A Practical Guide for Applying Techniques to Real-World Problems Computational Chemistry*, N.Y.: John Wiley & Sons, Inc., 2001.